Aging and Disease
www.aginganddisease.org
Early access date: January 24, 2026
http://dx.doi.org/10.14336/AD.2025.1307

Original Article

The α-MSH–MC1R Axis Modulates Sex-Specific Senescence and Inflammation Processes in Human Articular Chondrocytes and Mice Knee Joints

Nicole Schäfer[1], Paul Kalke[2], Ravikumar Mayakrishnan[3], Jian Mei[1], Luisa Kollatz[1], Marianne Ehrnsperger[4], Hadrian Platzer[3,5], Brian Johnstone[6], Arndt F. Schilling[2], Babak Moradi[3,5], Markus Böhm[7], Susanne Grässel[1*]

[1]Department of Orthopedic Surgery, Experimental Orthopedics, Centre for Medical Biotechnology (ZMB/Biopark 1), University of Regensburg, Germany. [2]Department of Trauma Surgery, Orthopedics and Plastic Surgery, University Medical Center Göttingen, Germany. [3]Orthopedic Research Center, Kiel University, Germany. [4]Department of Trauma Surgery, University Medical Center Regensburg, Regensburg, Germany. [5]Department of Orthopedics and Trauma Surgery, University Medical Center Schleswig-Holstein, Campus Kiel, Germany. [6]Department of Orthopedics and Rehabilitation, Oregon Health & Science University, Portland, Oregon, USA. [7]Department of Dermatology, University of Münster, Münster, Germany

[Received October 21, 2025; Revised January 2, 2026; Accepted January 2, 2026]

ABSTRACT: This study investigated the role of α-melanocyte-stimulating hormone (α-MSH) signaling in modulating sex-specific and inflammatory processes in aging related osteoarthritis (OA) models *in vitro* and *in vivo*. We aimed to determine if α-MSH elicits sex-dependent molecular effects on doxorubicin-induced senescence in OA and non-OA human chondrocytes *in vitro*, and to examine analogous sex-specific differences in senescence and inflammation in wild-type (WT) versus melanocortin receptor 1 (MC1R) signaling–deficient (MC1R$^{e/e}$) mice during aging. *In vitro*, human articular chondrocytes (hCh) from OA- and non-OA donors were subjected to doxorubicin-induced senescence and treated with Nle4-D-Phe7 (NDP)-α-MSH. Senescence markers (senescence-associated β-galactosidase (SA-β-gal), *CDKN2A*, *CDKN1A*), oxidative stress (reactive oxygen-, nitrogen species (ROS/RNS)), metabolic activity, secretion of matrix metalloproteinases (MMPs) and pro-inflammatory cytokine IL-6 were assessed. In parallel, in *in vivo* experiments, knee joint chondrocyte MC1R expression and apoptosis, as well as subchondral bone architecture, and synovial immune cell populations were analyzed in male and female WT and MC1R$^{e/e}$ mice aged up to 18 months. NDP-α-MSH partly mitigated doxorubicin-induced senescence markers and significantly reduced ROS/RNS levels in hCh. Effects were sex-specific and different between OA- and non-OA hCh *in vitro*. NDP-α-MSH also attenuated the secretion of pro-inflammatory IL-6 without affecting MMP secretion. *In vivo*, MC1R signaling deficiency in mice exacerbated spontaneous age-related processes in a sex-dependent manner, particularly in female mice, and influenced subchondral bone parameters and synovial immune cell profiles. α-MSH signaling plays a protective role during joint aging and OA associated cartilage and subchondral bone alterations by mitigating senescence, oxidative stress, and inflammation, with notable sex-specific differences. These findings emphasize the need for personalized and sex-based approaches and identify the α-MSH – MC1R axis as a potential therapeutic target for age-related disease-modifying interventions in OA.

Keywords: Melanocortin system, NDP-α-MSH, MC1R, cellular senescence, sex-dependent aging processes, osteoarthritis

***Correspondence should be addressed to:** Prof. Susanne Grässel, Department of Orthopedic Surgery, Experimental Orthopedics, Centre for Medical Biotechnology (ZMB/Biopark 1), Am Biopark 9, 93053 Regensburg, Germany. Email: susanne.graessel@ukr.de

INTRODUCTION

Aging is a multifactorial process marked by genomic instability, telomere shortening, epigenetic alterations, mitochondrial dysfunction, and altered intercellular communication. Senescent cells accumulate with age, defined by consistent cell-cycle arrest, enlarged morphology, and senescence-associated β-galactosidase (SA-β-gal) expression. Triggered by DNA damage and stress pathways, they remain metabolically active and adopt a senescence-associated secretory phenotype (SASP) rich in cytokines, chemokines, growth factors, and MMPs, which propagate senescence, drive inflammation, and promote matrix degradation. This secretory profile spreads senescence to neighboring cells and promotes chronic inflammation and extracellular matrix degradation, contributing to "inflammaging" [1–3].

Accumulation of senescent cells and SASP factors causes tissue deterioration and predisposes to age-related diseases such as osteoarthritis (OA). Senolytic strategies aim to selectively eliminate senescent cells or attenuate the SASP. Although seno-therapies have demonstrated promising effects in preclinical OA models, heterogeneity among senescent cells and concerns about long-term efficacy and safety highlight the need for careful translation [4].

OA is a heterogeneous, whole-joint disease affecting all joint tissues. Its pathology is driven by mechanical stress, metabolic and inflammatory factors, with age-related changes such as matrix stiffening, mitochondrial dysfunction, senescent chondrocytes, reactive oxygen species (ROS) production, cytokine release, and impaired autophagy contributing to degeneration. Shortly, OA develops through an interplay of mechanical stress, inflammatory and metabolic factors [5,6]. OA risks rise with age particularly in females, with women over 55 (around the menopause) experiencing higher prevalence, severity, and pain, partly linked to hormonal influences [7], obesity, joint anatomy and muscle strength [8,9]. Segal et al. found that 60% of subjects affected by OA were women, and that their perception of pain and radiological severity were higher compared to men. These findings correlated with the greater limitations of physical function and the increased need of analgesics in women, underscoring the need to integrate sex and gender in OA research and treatment [8].

Despite growing understanding of OA biology, treatments remain largely symptomatic – non-steroidal, anti-inflammatory drugs and corticosteroids relieve pain but do not halt structural damage. Joint replacement remains the ultimate remedy for the disease in its end-stage. The lack of disease-modifying OA drugs (DMOADs) underscores the need to explore novel therapeutic targets based on the biology of senescence and inflammation [9,10].

The melanocortin system comprises five G protein-coupled receptors (MC1R – MC5R), peptide agonists derived from proopiomelanocortin (POMC) – adrenocorticotropic hormone (ACTH), α-, β- and γ-melanocyte-stimulating hormones (MSHs) – and endogenous antagonists (agouti and agouti-related protein) [11]. Traditionally linked to pigmentation, melanocortin signaling also regulates energy balance, stress responses, and inflammation processes [12]. POMC-derived peptides, including ACTH and α-MSH are present in the synovial fluid, and ACTH plays a role in the differentiation of mesenchymal cells and regulation of bone mass among others. Moreover, MC1-5R are expressed in synovium, articular cartilage and bone [13]. This local expression suggests that melanocortin peptides can act in an autocrine/paracrine manner to regulate bone mineralization, cell proliferation and differentiation, extracellular matrix synthesis and immune responses in joint tissues.

Human articular chondrocytes (hCh) express MC1R, MC2R, and MC5R, and cartilage is recognized as a direct target of POMC-derived peptides [13]. Stimulation with α-MSH increases intracellular cyclic (c)AMP levels and alters mRNA- and protein expression of pro-inflammatory cytokines, collagens and MMPs, suggesting that hCh are important targets for melanocortin signaling [14]. α-MSH and ACTH reduce cytokine production, inhibit NF-κB-dependent transcription, and modulate leukocyte trafficking [15]. In joint tissues, α-MSH decreases synthesis of IL-6, IL-8 and MMP-1/-3 and promotes hCh homeostasis by increasing tissue inhibitor of metalloproteinases 3 (TIMP-3) expression. These actions align with the need to suppress synovitis and catabolic remodeling in OA. Besides, melanocortin pathways mediate female-specific effects on pain and κ-opiod related analgesia [16], supported by the known interactions between the melanocortin system, energy metabolism and reproductive hormones.

In 1993, Robbins et al. identified the *MC1R* gene as the murine extension locus, showing that the recessive yellow (e) allele produces a truncated, non-signaling receptor [17–19]. C57BL/6 mice homozygous for this allele ($MC1R^{e/e}$) lack functional signaling, have less cartilage, and upon OA induction by surgical medial meniscus destabilization, develop more severe cartilage erosion, osteophytes, and increased subchondral bone mass.

Overall, these data indicate that MC1R signaling is essential for preserving cartilage matrix integrity and limiting OA progression.

Therefore, we ask if sex-specific and age-related changes in melanocortin signaling shed light on

differences between male and females in aging and allows us to establish a basis for POMC/MSH-related, sex-specific therapies in age-associated diseases such as OA.

MATERIALS AND METHODS

Human samples

Human articular cartilage explants were obtained from knee joints of OA-patients after total knee replacement surgery (Asklepiosklinikum, Bad Abbach, Germany) and from healthy individuals through cadaveric donations of femoral condyles (OHSU, Portland, OR, USA), using leftover sections of clinically certified, pristine cartilage from osteochondral allografts. The use of human tissue was approved by the ethics committee at the University of Regensburg (ethics vote: 22-2915_1-101, ethikkommission@ur.de) (Supplementary Table 1).

Chondrocytes (hCh) were isolated as published previously [20]. They were cultivated using Dulbecco's Modified Eagle Medium (DMEM, Sigma-Aldrich, St. Louis, MO, USA) supplemented with 10% fetal bovine serum (FBS, Sigma-Aldrich, St. Louis, MO, USA) and 1% penicillin/streptomycin (Sigma-Aldrich, St. Louis, MO, USA) at 37 °C, 5% CO_2 and 95% humidity. Experimental setup was performed as shown in Supplementary Fig. 1. From the start of the experiment (day –1), hCh were cultured in chondrogenic medium containing DMEM high glucose (4.5 g/L, 1% pen/strep), recombinant human TGF-β3 (10 ng/mL, Sigma-Aldrich, St. Louis, MO, USA), dexamethasone (0.1 µM, Sigma-Aldrich, St. Louis, MO, USA), freshly prepared ascorbate-2-phosphate (50 µg/mL, Sigma-Aldrich, St. Louis, MO, USA), proline (40 µg/mL, Sigma-Aldrich, St. Louis, MO, USA), sodium pyruvate (110 µg/mL, Sigma-Aldrich, St. Louis, MO, USA), and ITS+ Premix Universal Culture Supplement (Omnilab, Bremen, Germany). hCh were subjected to the following treatment regimen: pre-treatment with NDP-α-MSH (1 µM, Tocris (Bio-Techne), Minneapolis, MN, USA, day 0), induction of senescence with doxorubicin (1 µM, Sigma-Aldrich, St. Louis, MO, USA, day 1), a second NDP-α-MSH treatment (1 µM, day 4), and subsequent *in vitro* analyses at day 7 (Supplementary Fig. 1). For all experiments, NDP-α-MSH, a synthetic analogue of α-MSH with enhanced potency and enzymatic stability, was used to provide a longer-lasting agonist effect compared to native α-MSH (21). For all experiments, chondrocytes at passage 1 and 2 were used.

Animals

Male and female Wild-type (WT) C57Bl/6J mice - serving as control animals - were purchased from Charles River Laboratories (Sulzfeld, Germany) at an age of 8 – 10 weeks and maintained under standard housing conditions, including a 12-hour light/dark cycle. Male and female $MC1R^{e/e}$ mice [17] were bred inhouse and maintained under the same standard housing conditions. Mice were euthanized at 6, 12 and 18 months. Food and water were available to all mice ad libitum.

RNA extraction and quantitative RT-PCR

Total RNA was extracted from hCh using the RNeasy Mini Kit (Qiagen, Venlo, The Netherlands, Cat. No. 74104) according to the manufacturer's protocol. RNA quality and integrity was assessed by a Bioanalyzer (Agilent, Santa Clara, CA, USA). Equal amounts of RNA were used for reverse transcription across all samples to ensure standardized cDNA synthesis, which was performed using the AffinityScript QPCR cDNA Synthesis Kit (Agilent Technologies, Waldbronn, Germany) following the manufacturer's protocol. Quantitative real-time PCR (qRT-PCR) was performed using Brilliant III Ultra-Fast SYBR QPCR (Agilent Technologies, Waldbronn, Germany) on an MX3005P QPCR System (Agilent, Santa Clara, CA, USA). Cycling conditions were as follows: initial denaturation at 95°C for 2 min, followed by 40 cycles of denaturation at 95°C for 5 s and annealing/extension at 60°C for 10 s. Relative gene expression levels were calculated using the ΔΔCt method and normalized to *HPRT1*, *TFRC* and *GAPDH* as internal reference genes (Supplementary Table 2). All qRT-PCR reactions were carried out in triplicates.

MC1R gene sequencing

Sequencing of the MC1R gene was performed using the Taqman SNP genotyping assay (ThermoFisher, Waltham, MA, USA). Each *MC1R* SNP was generated via the custom design tool. For the analysis of *MC1R* variants, 15 ng of DNA was used. Published *MC1R* variants are: p.V60L (rs1805005), p.D84E (rs1805006), p.V92M (rs2228479), p.R142H (rs11547464), p.R151C (rs180 5007), p.I155T (rs1110400), p.R163Q (rs885479), T314T (rs2228478) [22]. Mutant receptors with reduced cell surface expression and impairment in cAMP coupling (loss-of-function) are: V60L, D84E, R151C, I155T, R160W, R163Q [23]. Analyses of MC1R variants were performed according to the manufacturer's protocol using the following RT-PCR program: 1 × 95˚C/10 min; 40 × 92˚C/15 sec; 60˚C/60 sec; 4˚C/ cool down.

Cellular senescence – SA-ß-galactosidase assay

Senescence was assessed using a fluorometric SA-β-galactosidase assay (Cellular Senescence Assay Kit,

#CBA231, Cell Biolabs Inc.), which measures SA-β-gal activity in cell lysates and allows normalization across samples with varying cell numbers, according to the manufacturer's instructions. Fluorescence was measured with 360 nm excitation and 465 nm emission using ELISA Reader SpectraMax iD3 (Molecular Devices, Sunnyvale, CA, USA).

Reactive oxygen (ROS) and reactive nitrogen species (RNS)

Reactive oxygen/nitrogen species (ROS/RNS) levels were determined using the *OxiSelect™ In Vitro ROS/RNS Assay Kit* (Green Fluorescence; Hölzel Diagnostika, Köln, Germany) according to the manufacturer's protocol. Collected supernatants were stored at –80°C until use and diluted 1:7 in medium. Samples were centrifuged at 10,000xg for 5 min at 4°C prior to the assay. Fluorescence was measured using ELISA Reader SpectraMax iD3 (Molecular Devices, Sunnyvale, CA, USA).

Mitochondral dehydrogenase activity

Mitochondral dehydrogenase activity was assessed using the *WST-1 Assay Kit* (Abcam, Cambridge, UK; #ab65473) following the manufacturer's instructions. Briefly, $1x10^4$ cells were seeded in 100 µl F-12 medium without FCS in transparent 96-well plates (n=3). Subsequently, 10 µl of WST-1 reagent was added to each well, and the plates were incubated under standard culture conditions. After 1 h, absorbance was measured at 460 nm with a reference wavelength of 690 nm using ELISA Reader SpectraMax iD3 (Molecular Devices, Sunnyvale, CA, USA).

Metabolic activity/cell viability

Metabolic activity/cell viability was assessed using the *CellTiter-Glo® Luminescent Cell Viability Assay* (Promega, Madison, WI, USA; #G7570) according to the manufacturer's protocol with minor modifications. Briefly, $1x10^4$ cells were resuspended in 50 µl PBS (equivalent to 50,000 cells in 250 µl) and transferred into assay wells (n=3). An equal volume (50 µl) of CellTiter-Glo® reagent was added, and the samples were mixed on an orbital shaker for 2 min to ensure cell lysis. After incubation for 10 min at room temperature, luminescence was measured using ELISA Reader SpectraMax iD3 (Molecular Devices, Sunnyvale, CA, USA).

Luminex multiplex ELISA

Chondrocytes were cultivated and treated as previously described. Following incubation, supernatants were collected, analyzed, and stored at -80°C for long-term preservation. Luminex multiplex-ELISA of different proteins (Supplementary Table 3) was performed with cell supernatants (undiluted) using Bio-Plex 200 system with HTF (#171000205, Bio-Rad Laboratories, Hercules, CA, USA). The assays were performed according to the manufacturers' protocol.

Histology and immunohistochemistry of joint tissues

Following dissection, knee joints were fixed for 24 h in 4% paraformaldehyde/PBS and decalcified for 8 weeks in 20% EDTA (pH 7.4). After embedding in paraffin, 6 µm frontal sections were cut using a microtome. To assess cartilage deterioration, 12 sections (six adjacent pairs at intervals of 60–90 µm) were deparaffinized, rehydrated, and stained using Safranin O, Weigert's iron hematoxylin, and Fast Green. Two independent investigators, blinded to experimental conditions, evaluated the sections according to modified OARSI guidelines [24]. Immunhistochemistry was performed as published previously [25] with a polyclonal anti-MC1R antibody (final concentration 18 µg/ml, Origene Technologies, Rockville, MD, USA, #TA321479). TUNEL staining was performed using *Click-iT Plus TUNEL Assay* Alexa Fluor 647 (ThermoFisher, Waltham, MA, USA, #C10247), following the manufacturer's protocol. Digital images were captured using a BZ-X810 microscope (KEYENCE Deutschland GmbH, Neu-Isenburg, Germany) at 10x magnification. Mean OARSI scores from lateral and medial femoral condyles and tibial plateaus were calculated. MC1R- and TUNEL-positive cells were counted using QuPath open-source software [26]. Representative images were selected from the experimental group that best exemplified the median quantitative result for that group (Supplementary Fig. 2, 3).

To verify antibody specificity, isotype-matched controls, secondary antibody-only controls, and tissue sections known to be positive or negative for the respective targets were included in all immunostainings.

FACS analyses of synovial membranes

Synovial tissue pooled from 4 to 5 mice, aged 6 and 18 months, was finely minced and subjected to enzymatic digestion using Liberase TL (1 U/mL) for 60 min at 37 °C. The suspension was filtered through a 70–75 µm mesh, centrifuged at 300xg for 10 min, and resuspended in autoMACS® Running Buffer [27].

For surface staining, 2 µL of each fluorochrome-conjugated antibody was added to 100 µL of the cell

suspension in staining buffer. Viobility™ Fixable Dye (Miltenyi, 130-130-421) was used as a live/dead discriminator according to the manufacturer's instructions. Samples were incubated for 10 min at 4°C in the dark, diluted with 1 mL autoMACS buffer, centrifuged at 300xg for 10 min, and resuspended in 100 µL fresh autoMACS buffer. For intracellular staining (T-cell panel), surface-stained cells were fixed with Fixation Buffer from FoxP3 Staining Buffer Set (Miltenyi, 130-093-142) for 30 min at 4°C, washed, and permeabilized with Permeabilization Buffer for 10 min at 4°C. Cells were stained with antibodies against IL-17A, IL-4, CD25, and FoxP3 (2 µL each) for 30 min at 4°C in the dark, washed with autoMACS buffer, centrifuged, and resuspended for acquisition. Data were acquired using MACSQuant® 16 (Miltenyi Biotec) with standard compensation. Gating was performed sequentially on total cells → singlets → live cells, followed by lineage-specific analyses (Supp. Fig. 8). For lymphoid analyses, $CD3^+$ cells were gated as total T cells, with $CD3^+CD4^+$ cells defined as helper T cells and $CD3^+CD8^+$ cells as cytotoxic T cells. For myeloid analyses, gates were first restricted to non-lymphoid live singlets, after which $CD11b^+$ cells were identified as the total myeloid compartment. Within this population, neutrophils were defined as $CD11b^+Ly6G^+$, and tissue macrophages as $CD11b^+F4/80^+Ly6C^{\wedge}low$, using Ly6C expression to distinguish macrophages from Ly6C^high monocytes. All flow cytometry data were analyzed in FlowJo (BD), and cell frequencies are reported as proportions of the respective live-cell parent gates [27].

Nano-CT analysis of bone

The nano-CT analysis procedures employed in this study closely align with those outlined in our previous research [28–31]. Knee joints were harvested at 12 and 18 months and initially fixed in 4% paraformaldehyde (PFA) for 24 h. After fixation, the samples were preserved at 4°C in a 70% ethanol solution.

For imaging, the knee joints were scanned using a Scanco µCT 50 system (Scanco Medical, Brüttisellen, Switzerland) under ambient air conditions. The scanning parameters consisted of a source voltage of 90 kVp and a current of 88 µA. To mitigate beam hardening artifacts, a 0.50-mm aluminum filter was utilized. Each scan was performed with an isotropic voxel size of 6.8 µm and an integration time of 1000 ms, facilitating the generation of three-dimensional overviews of the femorotibial joint. This allowed for the evaluation of topographical modifications in the subarticular and epiphyseal region. Image reconstruction was executed using Scanco's OpenVMS software.

Bone morphometric indices were analyzed within two predefined volumes of interest (VOIs). The first VOI targeted the subarticular region, encompassing a 1.2 mm^3 area located 300 mm distal to the epiphyseal line, which was assessed for subarticular trabecular morphometry. The second VOI comprised an approximately 0.2 mm^3 region within the medial epiphysis, positioned between the inferior boundary of the subchondral bone plate and the epiphyseal line. In both VOIs, optimized threshold values for Scanco's OpenVMS software were applied (lower threshold: 685.3 mg HA/cm^3, upper threshold: 3000 mg HA/cm^3, Gauss Sigma: 0.8, Gauss Support: 1). Manual contouring was conducted while excluding the endocortical surface, in accordance with established guidelines.

Subchondral bone plate thickness was quantified using ImageJ software in three equidistant coronal cross-sections of the joint. The results for each condyle were presented as the mean ± SEM of 60 measurement points across the three coronal sections.

To analyze tibial plateau morphology, the lengths of the lateral and medial condyles were measured. These were defined as the distances from the condylar center near the trochlear groove to the respective lateral or medial prominence.

Mendelian randomization (MR) analysis

We conducted two-sample MR analyses to explore the causal effects of the *MC1R* gene on the risk of OA as published previously [32]. Single-nucleotide polymorphisms (SNPs)identified as *cis*-eQTLs for *MC1R* were extracted from the GTEx v8 European-ancestry eQTL database. Linkage disequilibrium (LD) clumping was applied (window size = 100 kb, $r^2 < 0.3$), and variants with a minor allele frequency (MAF) ≤ 0.01 were excluded. In this analysis, *MC1R* gene expression served as the exposure, whereas knee OA served as the outcome. Harmonized exposure and outcome datasets were analyzed using the Wald ratio method to estimate the causal effects, as each exposure ultimately retained only a single valid instrumental variable. All MR analyses were performed using the TwoSampleMR R package (v0.5.6). To further assess the robustness of the findings and determine whether the observed associations may be attributable to linkage rather than a true causal relationship, additional sensitivity analyses were performed using the Summary-data–based Mendelian Randomization (SMR) framework together with the HEIDI (Heterogeneity in Dependent Instruments) test (https://yanglab.westlake.edu.cn/smr-portal/). Detailed information regarding the data sources, instrumental variable characteristics, and sensitivity analyses is provided in the Supplementary Table 4a-c.

Statistical analysis

Data analysis and graphical representation were performed using GraphPad Prism version 10.5.0 (San Diego, CA, USA). Outlier detection was conducted with the ROUT method, setting Q=1% for OARSI scores and Q=5% for chondrocytes and supernatants data [33]. All *in vitro* data were analyzed using RM one-way ANOVA with Šídák's multiple comparisons test post hoc test to identify treatment- and sex-related differences. Differences in OARSI scores between groups based on genotype and age were assessed using Kruskal-Wallis tests followed by Dunn's multiple comparisons test. MC1R and TUNEL scores, Nano-CT and synovial immune cell data were analyzed by two-way ANOVA with Uncorrected Fisher's LSD post hoc test to identify genotype- and age-related differences. OARSI, MC1R and TUNEL scores are represented as box plots indicating medians with interquartile ranges and whiskers indicating minimum and maximum values. Nano-CT results are presented as bar graphs showing means ± standard deviations.

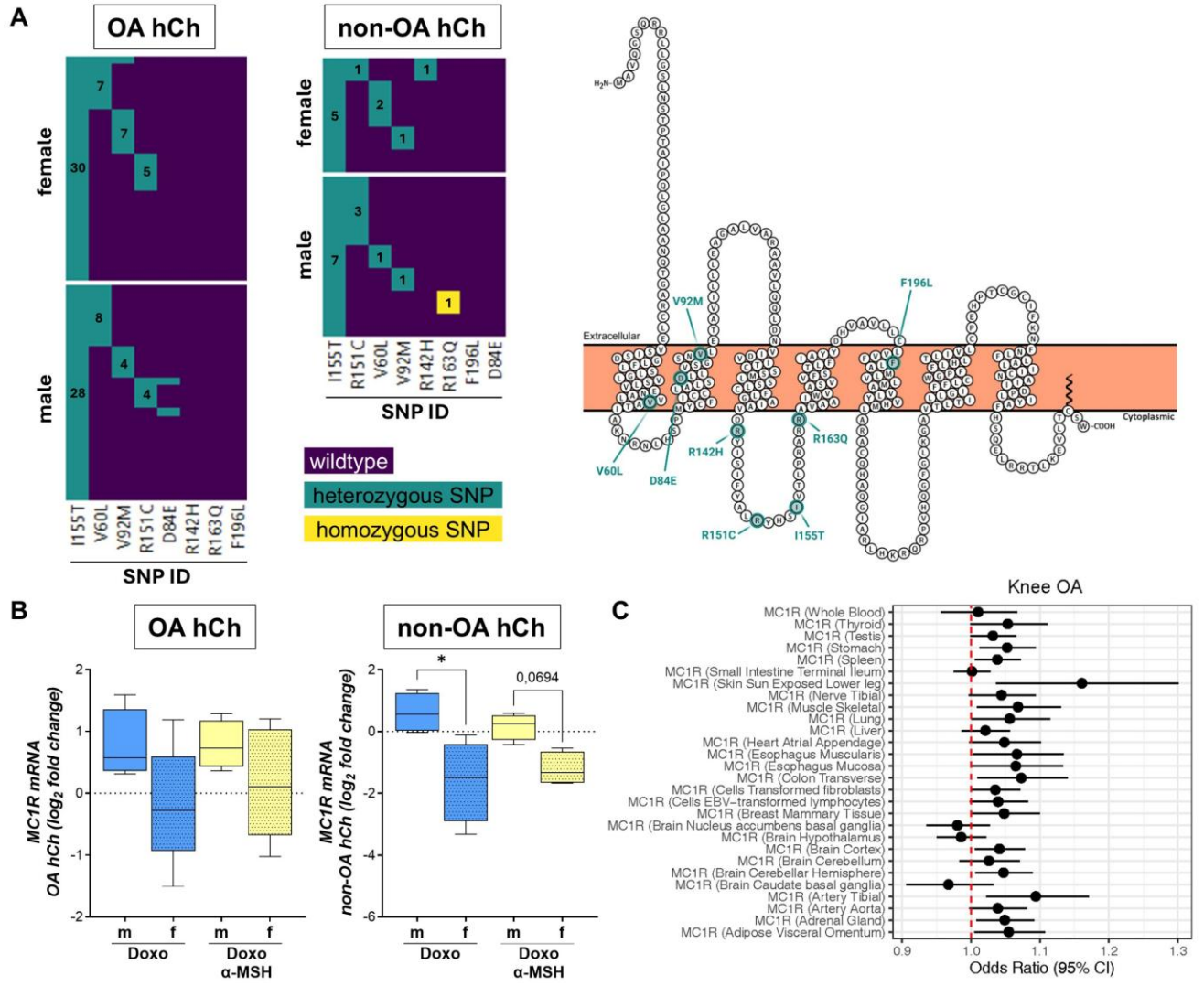

Figure 1. Genetic variants and *MC1R* mRNA expression in human articular chondrocytes. (A) Sex-specific *MC1R* gene sequencing results from OA- and non-OA hCh, highlighting wildtype (purple), heterozygous (green) and homozygous (yellow) single nucleotide polymorphisms (SNP). Numbers = donor numbers for each SNP. **(B)** *MC1R* mRNA expression levels in OA- and non-OA male and female hCh treated either with doxo (blue) or doxo combined with NDP-α-MSH (yellow) compared to untreated controls (0, dotted line). **(C)** Forest plot of Mendelian Randomization illustrating *MC1R* expression in different organs/tissues in knee OA. The higher the OR value the more likely is the biological relevance of the genetic correlation of the MC1R expression in the respective tissue. wildtype: these individuals do not contain one or more of the tested polymorphisms.

RESULTS

In this study we investigated the impact of α-MSH signaling on sex-specific senescence and inflammation processes in human articular chondrocytes (hCh) and mouse knee joints, integrating molecular and cellular *in vitro* analyses (Fig. 1 – 4), with *in vivo* outcomes (Fig. 5 – 8). We have used NDP-α-MSH in the *in vitro* part as it is superior in stability and potency compared to unmodified α-MSH.

Specifically, we tested whether NDP-α-MSH elicits sex-dependent molecular effects on doxorubicin (doxo)-induced senescence in OA- and non-OA hCh *in vitro*, and, in parallel, examined aging processes in knee joints of female and male wild-type versus MC1R signaling–deficient ($MC1R^{e/e}$) mice (6 – 18 months), particularly with respect to senescence and inflammation. For the *in vitro* analyses, Supplementary Figure 1A outlines the experimental timeline. We titrated NDP-α-MSH across concentrations from 0.01 to 1 µM and selected a two doses scheme with 1 µM NDP-α-MSH (administered on day 0 and day 4; Supplementary Fig. 1A) for all *in vitro* analyses, based on optimal outcomes and consistency with previous studies [14,34), using this equipotent concentration to match the maximal biological effect of native α-MSH while benefiting from the greater potency and enzymatic stability of NDP-α-MSH for our long-term *in vitro* assays. Baseline characterization of OA- and non-OA hCh responses to doxorubicin treatment comprised SA-β-gal activity (Supplementary Fig. 1B), caspase-3/7 activity (Supplementary Fig. 1C), and cell diameter with representative images (Supplementary Fig. 1D), establishing initial responses prior to experimental manipulation. We detected a comparable doxo-induced senescence and no apoptosis in OA- and non-OA hCh.

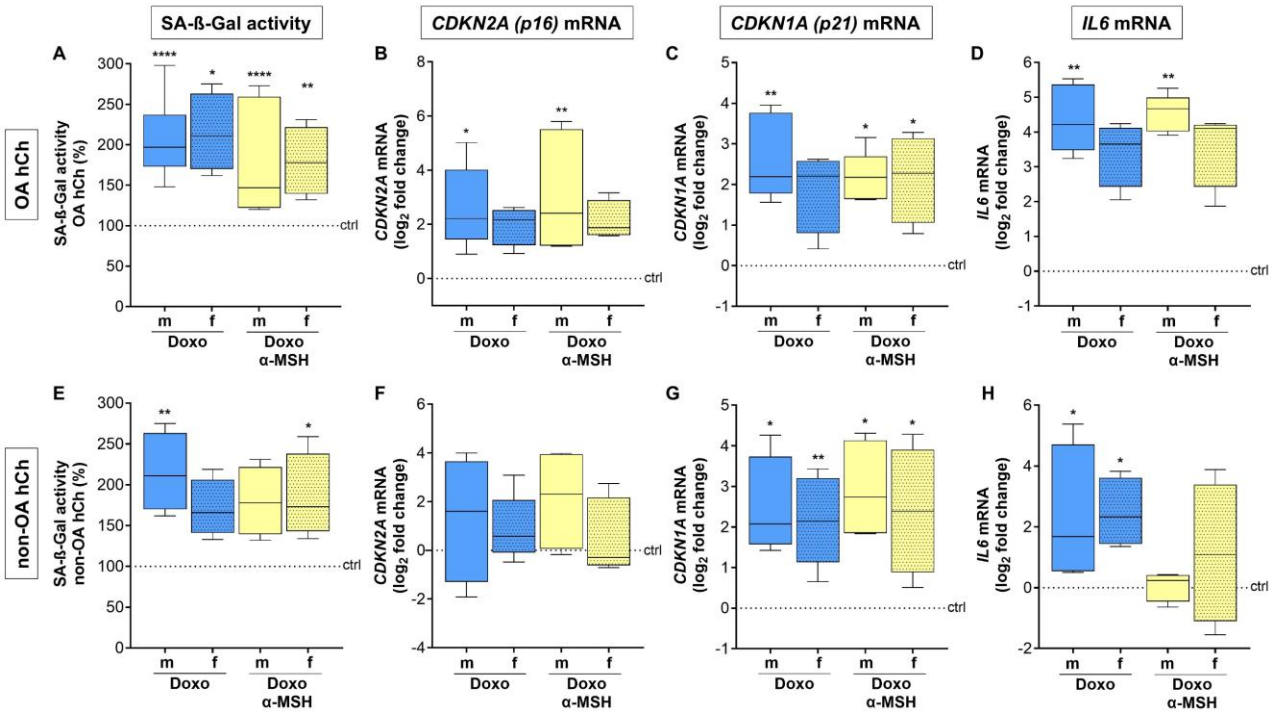

Figure 2. Impact of NDP- α-MSH on senescence markers in chondrocytes. (A, E) SA-β-gal activity in OA- (A) and non-OA (E) hCh, **(B, F)** mRNA expression levels of *CDKN2A* (p16) in OA- (**B**) and non-OA (**F**) hCh, **(C, G)** mRNA expression levels of *CDKN1A* (p21) in OA- (**C**) and non-OA (**G**) hCh, **(D, H)** mRNA expression levels of *IL-6* in OA- (**D**) and non-OA (**H**) hCh treated either with doxo (blue) or doxo and NDP- α-MSH (yellow) compared to untreated controls (0, dotted line); male hCh (m), female hCh (f). Statistical analysis was performed using non-parametric Kruskal-Wallis test followed by Dunn's post hoc test for multiple comparisons. * $p < 0.05$, ** $p < 0.01$, *** $p < 0.001$, **** $p < 0.0001$, N = 8 – 15, α-MSH = NDP-α-MSH

MC1R expression and genetic variants in human articular chondrocytes

We elucidated the genetic and expression profiles of MC1R in hCh, differentiating between sexes and OA- and non-OA samples. These findings are of fundamental relevance because the MC1R, a highly polymorphic G protein–coupled receptor (GPCR), shows gene variant-dependent functional differences that may modulate the anti-inflammatory actions of α-MSH, thereby contributing to OA pathogenesis [35). Fig. 1A presents the results of commonly known loss-of-function *MC1R*

missense mutations in OA (n = 58) and non-OA (n = 12) hCh using TaqMan® single nucleotide polymorphism (SNP) genotyping. All tested OA- and non-OA hCh were heterozygous for the *MC1R* variant I155T, and over 60% carried at least two heterozygous *MC1R* SNPs (Fig. 1A, green). One single non-OA hCh donor was homozygous for the mutation R163Q (Fig. 1A, yellow). Next, *MC1R* mRNA expression changes were measured in doxorubicin (doxo)- and doxo plus NDP-α-MSH-treated hCh. These treatments did not affect *MC1R* expression in OA hCh, however, sex-specific mRNA alterations were detected in non-OA hCh, with female donors exhibiting a significant *MC1R* transcript reduction relative to male donors (Fig. 1B). To determine if *MC1R* RNA expression is directly associated to knee OA, we applied Mendelian Randomization (MR) (Fig. 1C). This method uses genetic variants as natural indicators of how active a gene is, helping to separate the gene's true effect from other influences such as lifestyle or environmental factors. We combined data from two large-scale resources: the GTEx project to identify genetic *MC1R* variants predicting tissue-specific expression across multiple organs, and genome-wide association studies (GWAS) to evaluate the effect of these *MC1R* variants on knee OA risk. Results revealed consistent associations indicating that higher MC1R expression increases OA susceptibility. In summary, MR analysis uncovered tissue-specific causal effects of MC1R, with positive associations in sun-exposed skin and musculoskeletal tissues, contrasting with protective or neutral effects in distinct brain regions, underscoring the complex central – peripheral interactions through which MC1R may modulate OA pathophysiology. The widespread tissue signal suggests a systemic mechanism rather than a joint-localized effect and underscores the clinical relevance of the MC1R for knee OA (Fig. 1C). These genetic and expression data provide a basic understanding for the subsequent functional *in vitro* studies.

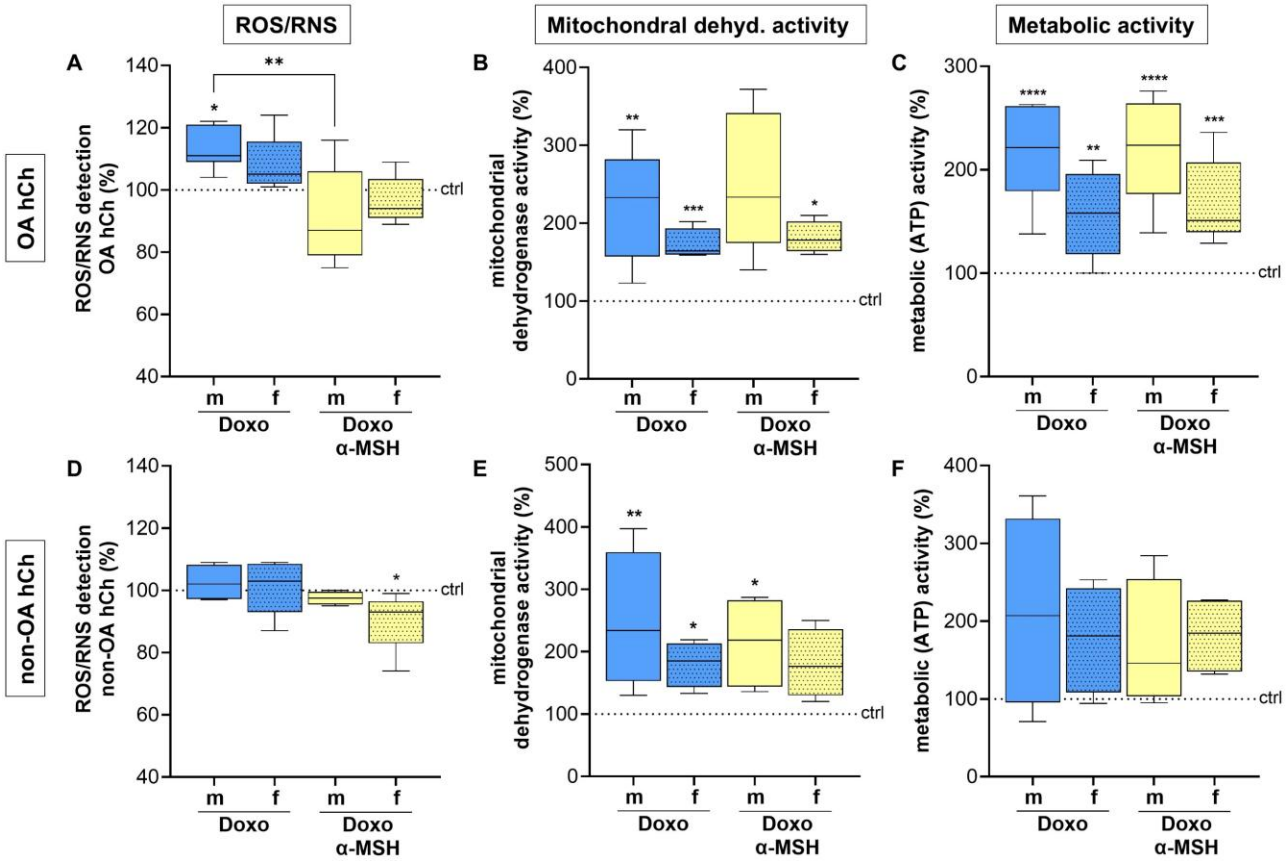

Figure 3. NDP-α-MSH modulates oxidative stress in chondrocytes. (A, D) Levels of Reactive Oxygen Species (ROS) and Reactive Nitrogen Species (RNS) in OA- (**A**) and non-OA (**D**) hCh. **(B, E)** Mitochondrial dehydrogenase activity in OA- (**B**) and non-OA **(E)** hCh, **(C, F)**. Overall metabolic activity (ATP) in OA- (**C**) and non-OA (**F**) hCh treated either with doxo (blue) or doxo and NDP- α-MSH (yellow) compared to untreated controls (dotted line); male hCh (m), female hCh (f). Statistical analysis was performed using non-parametric Kruskal-Wallis test followed by Dunn's post hoc test for multiple comparisons. * $p < 0.05$, ** $p < 0.01$, *** $p < 0.001$, **** $p < 0.0001$, N = 8 – 15, α-MSH = NDP-α-MSH

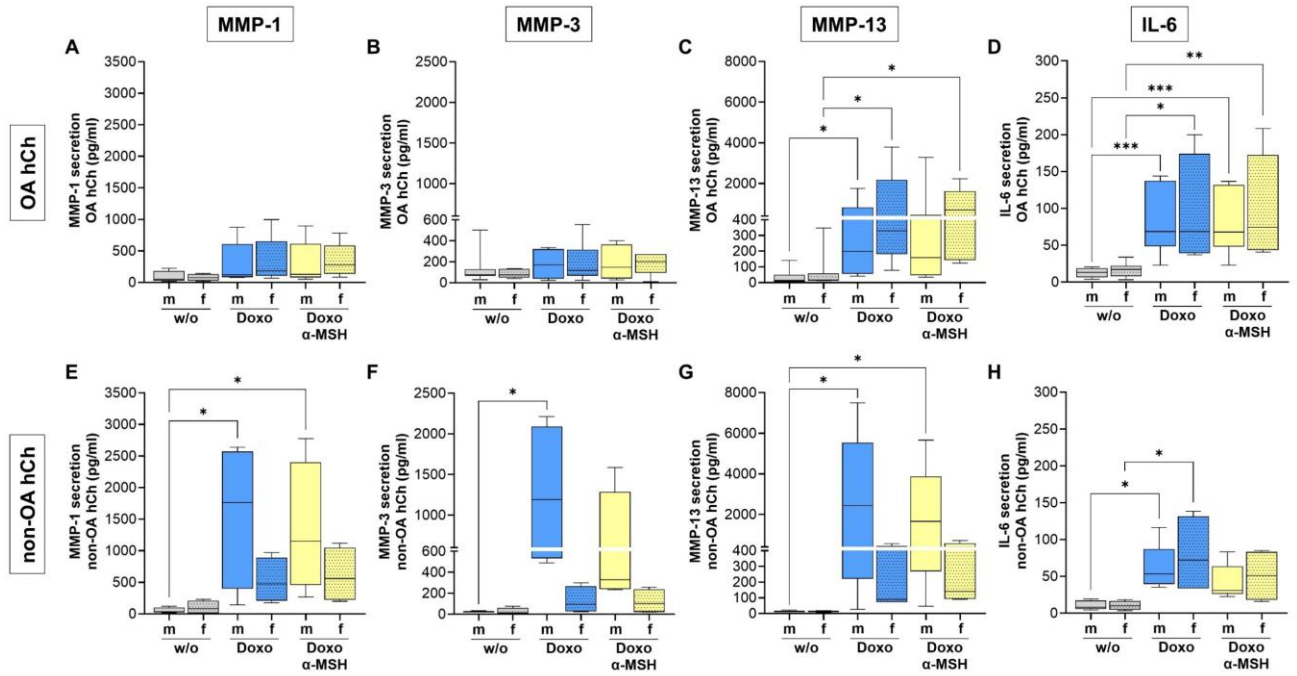

Figure 4. NDP-α-MSH effects on matrix metalloproteinase (MMP) and proinflammatory cytokine secretion. (A – C, E – G) Secretion levels of MMP-1, MMP-3, and MMP-13 in OA (**A – C**) and non-OA **(F – H**) hCh. **(D, H)** Secretion levels of Interleukin-6 (IL-6) in OA (**D**) and non-OA (**H)** hCh treated either with doxo (blue) or doxo and NDP- α-MSH (yellow) compared to untreated controls (grey); male hCh (m), female hCh (f). Statistical analysis was performed using non-parametric Kruskal-Wallis test followed by Dunn's post hoc test for multiple comparisons. * $p < 0.05$, ** $p < 0.01$, *** $p < 0.001$, **** $p < 0.0001$, N = 8 – 15, α-MSH = NDP-α-MSH.

Impact of NDP-α-MSH on senescence markers in human articular chondrocytes

Here, we investigated the effects of doxo-induced senescence and NDP-α-MSH treatment on key senescence markers in OA- (Fig. 2A – D) and non-OA hCh (Fig. 2E – H). SA-β-gal activity, a widely recognized biomarker for cellular senescence, was induced in both OA- (Fig. 2A) and non-OA hCh (Fig. 2E) after doxo-treatment. In non-OA male hCh, doxorubicin significantly increased SA-β-gal activity compared to control, and this increase was partially mitigated by NDP-α-MSH (Fig. 2E). This sex-specific effect was not observed in non-OA female hCh or in OA hCh of either sex, where NDP-α-MSH showed no significant effect. Next, mRNA expression levels of *CDKN2A (p16)* and *CDKN1A (p21)*, cyclin-dependent kinase inhibitors that play a crucial role in cell cycle arrest and senescence, were determined. In OA hCh, *CDKN2A* mRNA induction was specifically detected in male hCh after the treatments (Fig. 2B), with no statistically significant differences between sexes and no changes in non-OA cells (Fig. 2F). *CDKN1A* mRNA expression was elevated in male OA and non-OA hCh after both treatments and in female OA hCh after doxo+NDP-α-MSH treatment (Fig. 2C, G). However, the increase in female OA hCh after doxorubicin treatment alone was only increased by trend (Fig. 2C). Significant more transcripts of *IL6*, a prominent pro-inflammatory cytokine associated with the senescence-associated secretory phenotype (SASP), were observed in male OA- (Fig. 2D) and male/female non-OA (Fig. 2H) hCh following doxorubicin treatment, whereas NDP-α-MSH restored *IL6* mRNA levels to control values in non-OA cells of both sexes by trend (Fig. 2H) while this effect is lost in OA hCh (Fig. 2D). These data provide evidence for an anti-inflammatory potential of NDP-α-MSH in the context of cellular senescence, which is lost in OA.

Impact of NDP-α-MSH on oxidative stress and metabolic activity in human articular chondrocytes

We investigated the impact of doxorubicin and NDP-α-MSH on oxidative stress and metabolic parameters in OA- and non-OA hCh. Reactive Oxygen Species (ROS) and Reactive Nitrogen Species (RNS) are key indicators of oxidative stress. Doxorubicin induced ROS/RNS in male OA hCh, which was ameliorated by NDP-α-MSH (Fig. 3A); in female non-OA hCh, NDP-α-MSH even reduced ROS/RNS levels below untreated controls (Fig. 3D). Mitochondrial dehydrogenase activity is an indicator of

mitochondrial function and cell viability. Doxo treatment induced mitochondrial dehydrogenase activity in male and female OA and non-OA hCh (Fig. 3B, E). However, NDP-α-MSH did not affect doxo-induced mitochondrial function neither in OA- nor non-OA female and male hCh (Fig. 3B, E). Lastly, the overall metabolic activity was assessed by ATP release in response to the treatments. Metabolic activity increased in Doxo treated male and female OA hCh with no effect of NDP- α-MSH treatment or sex (Fig. 3C) whereas in non-OA samples no significant changes in ATP release was observed (Fig. 3F).

In summary, these results provide evidence that NDP-α-MSH partly counteracts doxorubicin-induced oxidative stress in OA sex-dependently and helps to maintain physiological oxidative levels. Of note, doxo does not induce oxidative stress in chondrocytes from healthy donors.

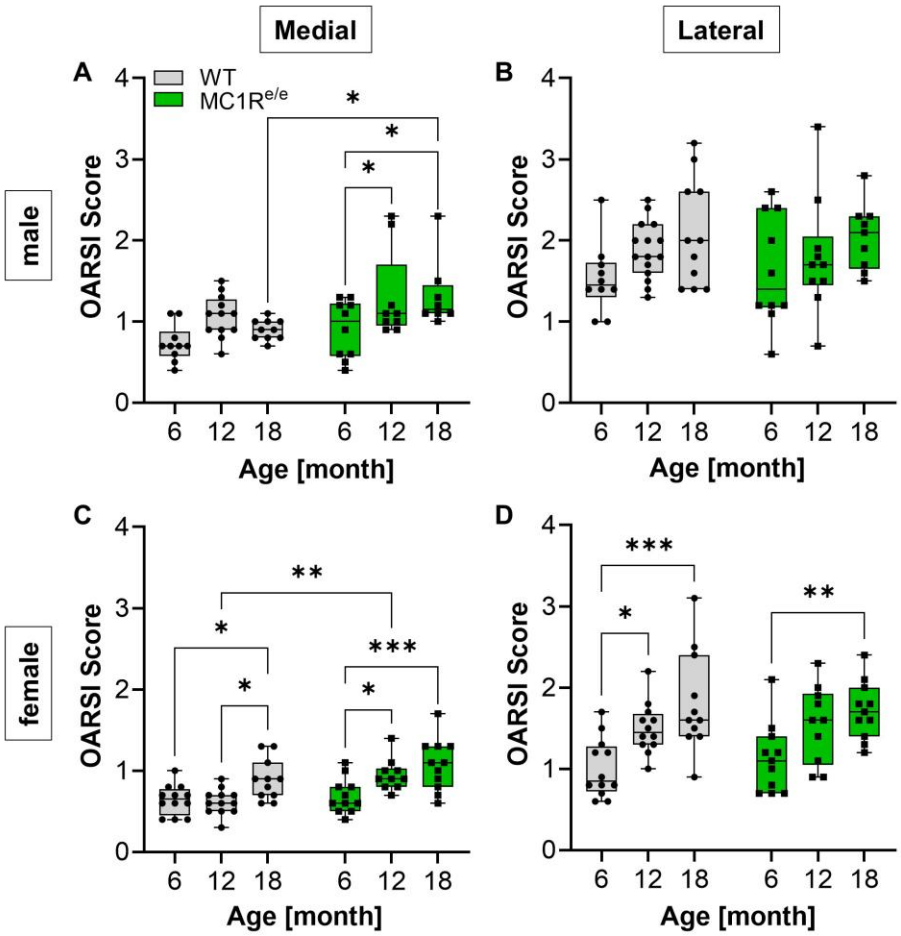

Figure 5. Differences in cartilage degradation during aging in MC1R$^{e/e}$ and WT mice. Cartilage was evaluated for grades of destruction according to the OARSI guidelines for murine OA. **(A, B)** OARSI scores for the medial and lateral compartments of knee joints in male WT (grey) and MC1R$^{e/e}$ (green) mice at 6, 12, and 18 months of age. **(C, D)** OARSI scores for the medial and lateral compartments of knee joints in female WT (grey) and MC1R$^{e/e}$ (green) mice at 6, 12, and 18 months of age. Statistical analysis was performed with Kruskal-Wallis and Dunn's test for multiple comparisons. * $p < 0.05$, ** $p < 0.01$, *** $p < 0.001$, N = 10 – 15.

Impact of NDP-α-MSH on sex-specific matrix metalloproteinase and IL-6 secretion in human articular chondrocytes

Here, we analyzed the effect of doxo- and NDP-α-MSH treatment on the secretion of MMPs and IL-6, crucial mediators of cartilage degradation and inflammation in aging and age-related diseases like OA. MMP-1 and -3 secretion was not affected by both treatments in OA hCh (Fig. 4A, B) whereas in non-OA hCh secretion of both MMPs was significantly increased in male samples only after doxo treatment with no effect of NDP-α-MSH treatment (Fig. 4E, F). MMP-13 secretion was doxo-dependent induced in male and female OA cells (Fig. 4C) and in male non-OA hCh only (Fig. 4G) with no further effect of NDP-α-MSH.

Secretion of pro-inflammatory IL-6 was doxo-dependent increased in female and male OA samples (Fig. 4D) and non-OA hCh with a slight mitigation by NDP-α-MSH in non-OA hCh (Fig. 4H). This analysis underscores the potent sex-dependent catabolic and inflammatory effects of doxo-induced senescence on hCh with a mild impact of NDP-α-MSH.

Sex- and genotype-specific differences in murine cartilage degeneration during aging

Our *in vivo* investigations were performed with adult WT- and MC1R$^{e/e}$ mice to elucidate the role of MC1R signalling in spontaneous aging processes, with a particular focus on sex-specific differences and aging-associated OA like cartilage and subchondral bone changes.

The OARSI scoring system was employed to assess cartilage degeneration for the medial and lateral compartments of knee joints in male and female WT and MC1R$^{e/e}$ mice at 6, 12, and 18 months (Fig. 5). The OARSI scores increased significantly in the medial compartment for male MC1R$^{e/e}$ mice with increasing age and a significant increase compared to male WT at 18 months. Scores of male WT mice remained low and did not increase up to 18 months (Fig. 5A). The lateral compartment was not affected by genotype and increasing age, however, showed overall higher scores than the medial compartment (Fig. 5B). The OARSI scores for female mice increased significantly age-dependent in both compartments (Fig. 5C, D) with a significant higher score for MC1R$^{e/e}$ mice compared with WT at the age of 12 months in the medial compartment (Fig. 5C).

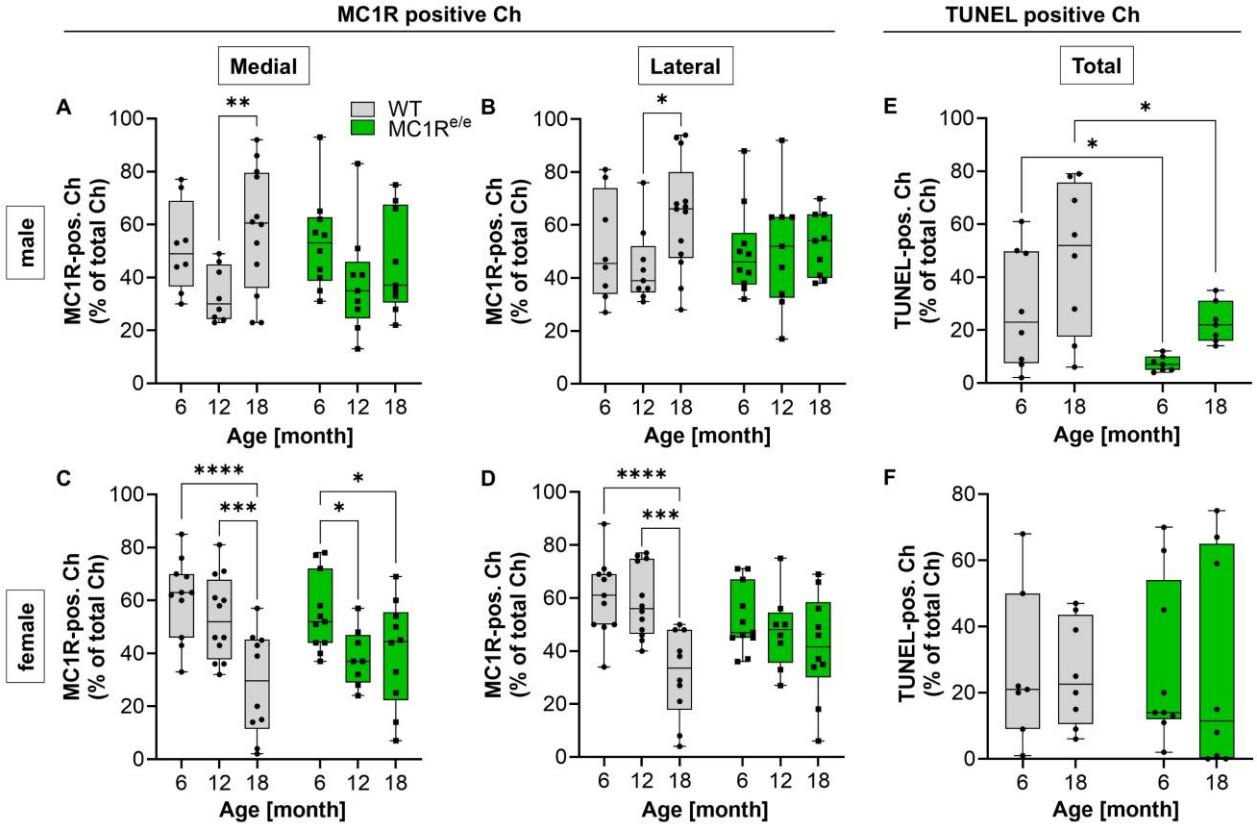

Figure 6. MC1R expression and apoptotic chondrocytes in MC1R$^{e/e}$ compared to WT mice. (A, B) Percentage of MC1R-positive chondrocytes in the medial and lateral knee compartments of male WT and MC1R$^{e/e}$ mice at 6, 12, and 18 months. **(C, D)** Percentage of MC1R-positive chondrocytes in the medial and lateral knee compartments of female WT and MC1R$^{e/e}$ mice at 6, 12, and 18 months. **(E, F)** Percentage of TUNEL-positive chondrocytes in both compartments of knee joints of male and female WT and MC1R$^{e/e}$ mice at 6, and 18 months, indicating apoptotic cell death. Statistical analysis was performed with two-way ANOVA with Uncorrected Fisher's LSD post hoc test. * $p < 0.05$, ** $p < 0.01$, *** $p < 0.001$, **** $p < 0.0001$, N = 8 – 13

These findings provide evidence that MC1R signaling deficiency can influence the severity and progression of cartilage degeneration in a sex- and age-dependent manner. Of note, males are partly protected from cartilage degeneration, which is lost when MC1R signaling is abolished.

Sex- and genotype-specific differences in murine chondrocyte apoptosis and MC1R expression during aging

Further analysis characterized the cellular changes within the articular knee cartilage, focusing on chondrocyte MC1R protein expression (Fig. 6A-D, Supplementary Fig. 2) and apoptosis (Fig. 6E, F, Supplementary Fig. 3).

MC1R-positive chondrocytes were quantified compared to total chondrocyte numbers in the medial and lateral knee compartments of male and female WT and MC1R$^{e/e}$ mice at 6, 12 and 18 months. While male WT mice exhibited an age-dependent increase in MC1R positive chondrocytes in both compartments (Fig. 6A, B), in female WT MC1R positive chondrocytes decreased with age (Fig. 6C, D). The number of MC1R positive chondrocytes in MC1R$^{e/e}$ mice did not change significantly except for an age-associated decrease in the medial compartment of female mice. These data provide evidence of MC1R presence within knee cartilage during aging and sex-dependent alterations in its expression with female mice loosing MC1R protein and male mice increasing its expression.

TUNEL-positive chondrocytes, indicative of apoptotic cells, were determined in the knee joints of male and female WT and MC1R$^{e/e}$ mice at 6 and 18 months. Male WT mice had more apoptotic cells than MC1R$^{e/e}$ mice at both ages (Fig. 6E), whereas no difference in numbers were observed in females due to a high variability in MC1R$^{e/e}$ mice at both ages (Fig. 6F). These findings further support a sex-dependent, MC1R-associated effect in aging murine chondrocytes.

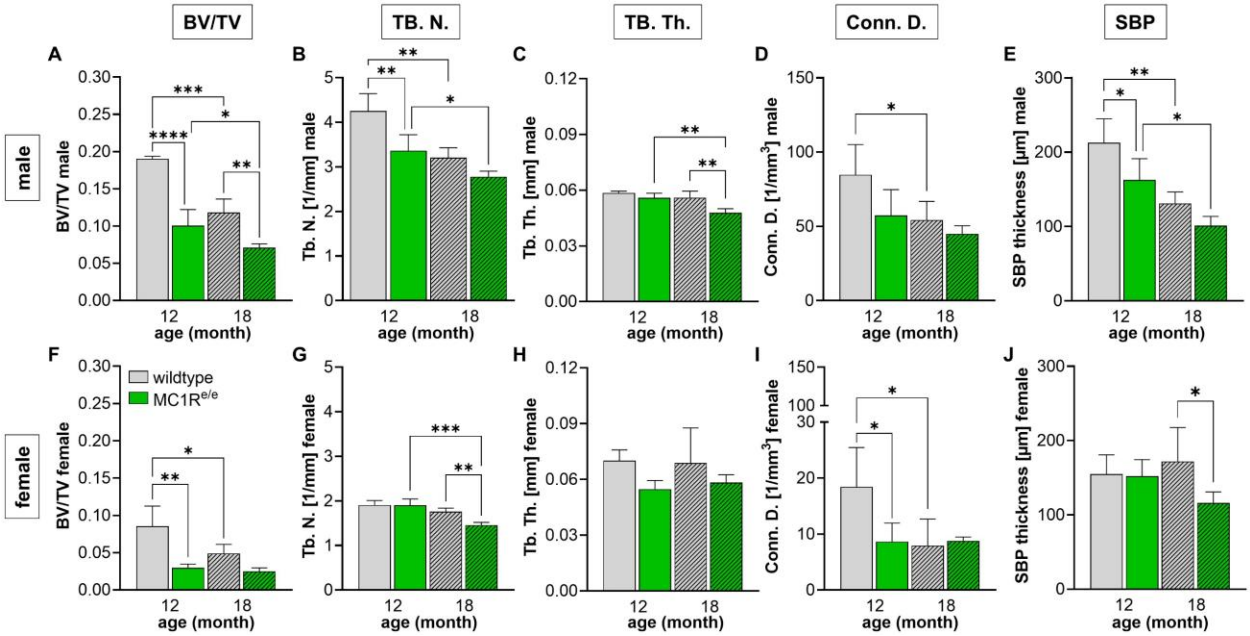

Figure 7. Subchondral bone morphology parameter in MC1R$^{e/e}$ compared to WT mice. Ultra-high resolution nano-CT analysis of medial subchondral bone morphology: bone volume/total volume (BV/TV), trabecular number (Tb.N.), trabecular thickness (Tb.Th.), connectivity density (Conn.D.) and subchondral bone plate thickness (SBP) in male **(A – E)** and female **(F – J)** wild-type (WT, grey) and MC1R$^{e/e}$ (green) mice at 12 and 18 months. Statistical analysis was assessed using two-way ANOVA with Uncorrected Fisher's LSD post hoc test. * $p < 0.05$, ** $p < 0.01$, *** $p < 0.001$, **** $p < 0.0001$, N = 3 – 4.

Sex- and genotype-specific differences in murine subchondral bone morphology during aging

The following results address the subchondral bone architecture, a key determinant of joint health and OA pathology, in male and female WT and MC1R$^{e/e}$ mice at 12 and 18 months. Bone volume/total volume (BV/TV, Fig. 7A, F), trabecular number (Tb.N., Fig. 7B, G), trabecular thickness (Tb.Th., Fig. 7C, H), connectivity density (Conn.D., Fig. 7D, I), and subchondral bone plate thickness (SBP, Fig. 7E, J) decreased overall with age in both genotypes (except for Tb.Th. which only decreased in MC1R$^{e/e}$ mice), but particularly obvious in male mice. In female mice, age- and genotype associated changes were less obvious. Overall, subchondral bone parameters (except for Tb.Th.) showed lower values in females than in males. In contrast, bone surface (BS, Supplementary Fig. 4A, D) and bone volume (BV, Supplementary Fig. 4B, E) increased with age mostly in MC1R$^{e/e}$ mutants, without sex-specific differences (Supplementary Fig. 4). Representative nano-CT images of SBP and subarticular bone are depicted in Supplementary Figure 5 and 6.

These data reveal the impact of MC1R signaling deficiency on bone remodeling and integrity in a sex- and age-specific manner, suggesting a critical role for MC1R signalling in maintaining subchondral bone homeostasis during aging.

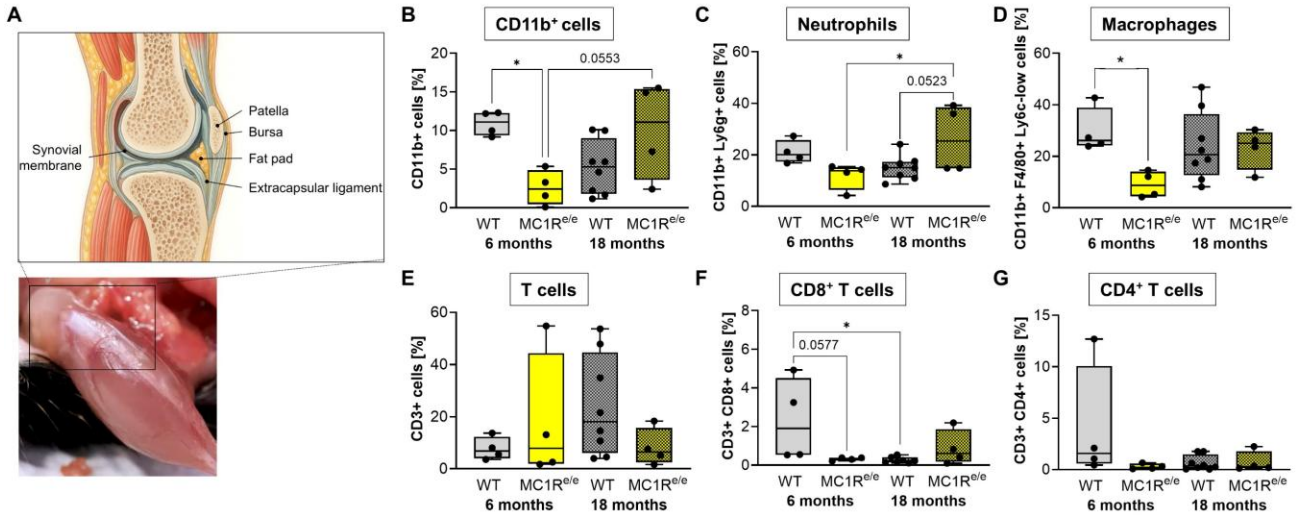

Figure 8. Synovial immune cell populations in female MC1R$^{e/e}$ compared to WT mice. Flow cytometry analysis shows the percentages of various synovial immune cell populations in female WT (grey) and MC1R$^{e/e}$ (yellow) mice at 6 and 18 months. **(A)** Shows mouse knee synovial tissues analyzed by FACS for synovial immune cells. **(B – D)** Represent myeloid-lineage of total CD11b+ cells and within that population separately neutrophils and macrophages, whereas **(E – G)** depict total T cells, and within that population separately CD4+ and CD8+ T cells. Statistical analysis was assessed using two-way ANOVA with Uncorrected Fisher's LSD post hoc test. * $p < 0.05$, $N = 4 – 8$.

Sex-specific differences in synovial immune cell populations of WT and MC1R$^{e/e}$ mice

Finally, a cell type-specific flow cytometry analysis (FACS) of synovial immune cell populations was performed, offering insights into the inflammatory status of the joint in the context of MC1R signaling deficiency and aging (Fig. 8, Supplementary Fig. 7 and 8). Percentages of several synovial immune cell subsets from WT and MC1R$^{e/e}$ mice at 6 and 18 months of age, including CD11b^{+} cells, neutrophils, macrophages and T cells, were counted (36,37) (Fig. 8A). CD11b+ cells and neutrophils increased with age in female MC1R$^{e/e}$ mice (Fig. 8B, C), while at 6 months these mice had fewer CD11b^{+} cells, specifically macrophages, than WT (Fig. 8B, D). For T cell analysis (Fig. 8E-G) in aged female WT mice fewer CD4^{+}/8^{+} T cells than in 6 months mice were counted (Fig. 8F), whereas no clear age-related changes were detectable for MC1R$^{e/e}$ mice. No equivalent cell count changes were observed in male WT and MC1R$^{e/e}$ mice (Supplementary Fig. 7). Immune cell profiling is crucial for understanding the underlying mechanisms by which MC1R signaling modulates joint inflammation and provides further evidence for its involvement in the synovial immune response within the joint.

DISCUSSION

OA is a multifactorial joint disease driven not only by mechanical stress but also by systemic aging processes [5,6]. One of the key factors is the accumulation of senescent cells, which secrete pro-inflammatory SASP that promote chronic inflammation, matrix degradation, and pathological tissue remodeling [1,2,38]. In addition to senescent chondrocytes, senescent fibroblast-like synoviocytes in the osteoarthritic joint also promote OA progression. Synovial fibroblasts, synovial macrophages, osteoblasts and adipocytes are involved in the production of SASPs in addition to chondrocytes during aging in the joint thereby contributing directly to cartilage loss and subchondral bone changes in OA [39].

Our study provides evidence that α-MSH-MC1R signaling plays a critical role in modulating sex-specific senescence and inflammatory processes in human articular chondrocytes and in aging processes in mice, thereby highlighting its potential as a novel therapeutic target. The initial investigations into MC1R expression and genetic variants in OA- and non-OA hCh revealed differential expression patterns and the presence of various heterozygous SNPs in both OA- and non-OA cells and one homozygous SNP in non-OA samples. This finding is particularly important as the MC1R is known to mediate the anti-inflammatory effects of α-MSH and related peptides [15,40]. Alterations in MC1R expression or function, as suggested by the detected SNPs, could compromise the endogenous protective mechanisms mediated by α-MSH, thereby contributing to OA pathogenesis. The Mendelian Randomization analysis further underscored the clinical relevance of MC1R gene expression in knee OA, aligning with previous studies that

have implicated melanocortin signaling in joint homeostasis and pathology [13,14,34]. These genetic and expression data provide a foundational understanding of the results of subsequent functional studies.

The *in vitro* experiments demonstrated some impact of NDP-α-MSH on senescence markers in hCh. Doxorubicin-induced senescence, characterized by increased SA-β-gal activity and elevated expression of cell cycle inhibitors like p16 (*CDKN2A*) and p21 (*CDKN1A*), was not mitigated by NDP-α-MSH treatment. This is a critical finding, as cellular senescence in chondrocytes is increasingly recognized as a key driver of OA progression, contributing to matrix degradation and inflammation through SASP [5,39]. However, the reduction in *IL6* mRNA expression and partly secretion by NDP-α-MSH, especially detected in senescent non-OA hCh, supports the anti-inflammatory and anti-senescent properties of NDP-α-MSH, These results are consistent with prior research showing that α-MSH and activation of MC1,-2 and -5Rs can reduce release of pro-inflammatory cytokines and support chondrocyte homeostasis [41–43].

Beyond senescence, our study revealed that NDP-α-MSH effectively modulates oxidative stress in hCh. Doxorubicin increased ROS/RNS levels, mitochondrial dehydrogenase activity, and metabolic activity, particularly in OA hCh, with a trend toward stronger responses in males, suggesting sex-dependent oxidative stress and mitochondrial dysfunction. Those are well-established contributors to OA pathology and are intimately linked to the aging process and the induction of senescence [44,45]. NDP-α-MSH treatment significantly ameliorated oxidative stress effects, highlighting its antioxidant capabilities. This is particularly relevant given that oxidative stress can trigger inflammatory cascades and accelerate chondrocyte apoptosis, further exacerbating age-related joint degeneration [44].

Furthermore, our findings demonstrate that senescence induction promotes the secretion of key matrix metalloproteinases (MMPs) and IL-6 in a sex-dependent manner with overall higher secretion levels in males than females. MMP-1, MMP-3, and in particular MMP-13 as components of SASP are central to the enzymatic breakdown of the extracellular matrix in articular cartilage, and their elevated levels are hallmarks of OA [46,47]. However, NDP-α-MSH treatment elicited only weak effects. These findings contrast with previous reports showing that NDP-α-MSH down modulates cytokine-induced responses and inhibits NF-κB-dependent transcription to promote matrix preservation [41–43], raising the question of whether the identified MC1R SNPs might contribute to the limited effects of NDP-α-MSH.

Our *in vivo* studies using MC1R$^{e/e}$ mice provided insights into the role of MC1R in aging associated with OA-like processes in the knee joints and revealed significant sex-specific differences. The observed exacerbation of degradative processes in knee cartilage and subchondral bone in MC1R$^{e/e}$ mice in a sex-dependent manner, suggests that endogenous MC1R signaling plays a protective role in maintaining joint health. This aligns with translational studies indicating an inverse correlation between synovial fluid α-MSH levels and OA severity in humans [48–50]. Further analysis of cellular changes within the articular cartilage, focusing on MC1R protein expression and chondrocyte apoptosis, revealed age- and sex-dependent alterations. The age-dependent increase in MC1R expression in chondrocytes in male WT mice, contrasting with lower expression in female WT chondrocytes, suggests a complex interplay between sex, aging, and MC1R signaling in cartilage homeostasis. The observation that male WT mice contained more apoptotic chondrocytes than MC1R$^{e/e}$ mice at both 6 and 18 months, while no differences were observed in females, further supports a sex-dependent, MC1R-mediated effect of aging on cartilage. Chondrocyte apoptosis is a critical event in OA pathogenesis, contributing to cell loss and subsequent cartilage matrix degradation, a process often accelerated in the aging joint [51]. The protective role of MC1R signaling against apoptosis, particularly in males, highlights a potential mechanism by which this pathway preserves chondrocyte viability during aging and might contribute to a higher OA prevalence in females.

Subchondral bone architecture, a key determinant of joint health and OA pathology, also exhibited age- and sex-dependent changes influenced by MC1R signaling deficiency. Parameters such as bone volume/total volume (BV/TV), trabecular number (Tb.N.), trabecular thickness (Tb.Th.), connectivity density (Conn.D.), and subchondral bone plate (SBP) thickness decreased with age, clearly stronger in MC1R$^{e/e}$ mutant mice. Overall, reduced bone volume, trabecular structure, and SBP thickness, particularly in female MC1R$^{e/e}$ mice – align with reports that women have a higher knee OA prevalence than men [8,52]. These findings underscore the broader systemic and sex-dependent role for the melanocortin system in maintaining musculoskeletal homeostasis, extending beyond cartilage to subchondral bone, which is subject to age-related deterioration and contributes to OA progression [28–30]. The interplay between cartilage and subchondral bone is crucial for proper joint function, and age-related changes in bone quality can significantly impact joint mechanics and progression of OA.

Finally, FACS analysis of synovial immune cell populations offered insights into the inflammatory status of the joint in the context of MC1R signaling deficiency. The age-dependent increase in CD11b^{+} cells in MC1R$^{e/e}$

mice, alongside differences in $CD8^+$ T cell numbers, provides evidence for the involvement of MC1R in modulating the immune response within the joint. Chronic low-grade inflammation, or inflammaging, is a hallmark of aging and a significant contributor to OA pathogenesis [38,53]. The observed alterations in immune cell populations in $MC1R^{e/e}$ mice suggest that MC1R signaling plays a role in regulating this age-related inflammatory response, potentially by modulating the recruitment or activation of immune cells within the synovial environment.

Conclusions

Collectively, our findings strengthen the understanding of α-MSH signaling as a regulator of joint health, particularly in the context of sex-dependent aging and aging-related diseases as OA. The ability of NDP-α-MSH to partially counteract cellular senescence, oxidative stress, and the production of inflammatory mediators in chondrocytes positions it as a potential therapeutic target. Furthermore, the sex-specific influence of MC1R deficiency on aging and OA-related processes in mice underscores the physiological relevance of this pathway and highlights the importance of personalized approaches in future therapies of aging related joint diseases.

Limitations

This study provides important insights into the sex-specific role of NDP-α-MSH and the MC1R signaling axis in aging and OA development, yet several limitations should be considered. The *in vitro* experiments relied on 2D cultures and doxorubicin-induced senescence, which do not fully reflect the 3D joint microenvironment or natural aging/OA stressors, highlighting the need for more physiological models. While the aged $MC1R^{e/e}$ mouse model offered pathophysiological insights, it represents a genetic system that cannot capture the multifactorial nature of human aging and OA development, with the observed sex-specific effects needing further mechanistic investigations. Moreover, the downstream pathways of α-MSH signaling remain to be defined, and future studies should employ pathway-specific tools, post-traumatic OA models, and *in vivo* analyses of dosage, timing, and delivery strategies to enable clinical translation. As a final limitation, the OA- and non-OA cohorts differed significantly in age ($P < 0.0001$). Therefore, age may act as a confounder and should be considered when interpreting between-group comparisons.

Acknowledgements

This project was supported by the German Research Foundation (Deutsche Forschungsgemeinschaft (DFG): BO-1075/12-3; GR 1301/22-1 (common grant: MB and SG); SCHI 857/9-2 (PK and AFS). We thank Claudia Göttl, Maren Hofmann and Anja Pasoldt for excellent technical support.

Author contributions

Conceptualization: NS and SG. Data curation: NS. Formal analysis: NS. Funding acquisition: MB and SG. Investigation: NS and SG. Methodology: NS, PK, JM, RM, LK. Project administration: NS and SG. Supervision: SG. Visualization: NS. Writing – original draft: NS. Writing – review and editing: all authors. All authors have read and agreed to the published version of the manuscript.

Competing interests

The authors declare that the research was conducted in the absence of any commercial or financial relationships that could be construed as a potential conflict of interest.

Data and materials availability

The datasets used and/or analyzed during the current study are available from the corresponding author on reasonable request.

Supplementary Materials

The Supplementary data can be found online at: www.aginganddisease.org/EN/10.14336/AD.2025.1307.

References

[1] Zhang L, Pitcher LE, Yousefzadeh MJ, Niedernhofer LJ, Robbins PD, Zhu Y (2022). Cellular senescence: a key therapeutic target in aging and diseases. J Clin Invest, 132(15):e158450.

[2] Mylonas A, O'Loghlen A (2022). Cellular Senescence and Ageing: Mechanisms and Interventions. Front Aging, 3:866718.

[3] Batushansky A, Zhu S, Komaravolu RK, South S, Mehta-D'souza P, Griffin TM (2022). Fundamentals of OA. An initiative of Osteoarthritis and Cartilage. Obesity and metabolic factors in OA. Osteoarthris Cartilage, 30(4):501–15.

[4] Astrike-Davis EM, Coryell P, Loeser RF (2022). Targeting cellular senescence as a novel treatment for osteoarthritis. Curr Opin Pharmacol, 64:102213.

[5] Coaccioli S, Sarzi-Puttini P, Zis P, Rinonapoli G, Varrassi G (2022). Osteoarthritis: New Insight on Its Pathophysiology. J Clin Med,11(20):6013.
[6] Roelofs AJ, De Bari C. Osteoarthritis year in review 2023: Biology (2024). Osteoarthritis Cartilage, 32(2):148–58.
[7] Dennison EM (2022). Osteoarthritis: The importance of hormonal status in midlife women. Maturitas, 165:8–11.
[8] Segal NA, Nilges JM, Oo WM (2024). Sex differences in osteoarthritis prevalence, pain perception, physical function and therapeutics. Osteoarthritis Cartilage, 32(9):1045–53.
[9] Courties A, Kouki I, Soliman N, Mathieu S, Sellam J (2024). Osteoarthritis year in review 2024: Epidemiology and therapy. Osteoarthritis Cartilage, 32(11):1397–404.
[10] Schäfer N, Grässel S (2022). Targeted therapy for osteoarthritis: progress and pitfalls. Nat Med, 28(12):2473–5.
[11] Cone RD (2006). Studies on the physiological functions of the melanocortin system. Endocr Rev, 27(7):736–49.
[12] Dinparastisaleh R, Mirsaeidi M (2021). Antifibrotic and Anti-Inflammatory Actions of α-Melanocytic Hormone: New Roles for an Old Player. Pharmaceuticals (Basel), 14(1):1–20.
[13] Böhm M, Grässel S (2012). Role of proopiomelanocortin-derived peptides and their receptors in the osteoarticular system: From basic to translational research. Endocr Rev, 33(4):623–51.
[14] Grässel S, Opolka A, Anders S, Straub RH, Grifka J, Luger TA,Böhm M (2009). The melanocortin system in articular chondrocytes: Melanocortin receptors, pro-opiomelanocortin, precursor proteases, and a regulatory effect of α-melanocyte-stimulating hormone on proinflammatory cytokines and extracellular matrix components. Arthritis Rheum, 60(10):3017–27.
[15] Brzoska T, Luger TA, Maaser C, Abels C, Böhm M (2008). Alpha-melanocyte-stimulating hormone and related tripeptides: biochemistry, antiinflammatory and protective effects in vitro and in vivo, and future perspectives for the treatment of immune-mediated inflammatory diseases. Endocr Rev, 29(5):581–602.
[16] Mogil JS, Wilson SG, Chesler EJ, Rankin AL, Nemmani KVS, Lariviere WR, et al (2003). The melanocortin-1 receptor gene mediates female-specific mechanisms of analgesia in mice and humans. Proc Natl Acad Sci USA, 100(8):4867–72.
[17] Robbins LS, Nadeau JH, Johnson KR, Kelly MA, Roselli-Rehfuss L, Baack E, et al (1993). Pigmentation phenotypes of variant extension locus alleles result from point mutations that alter MSH receptor function. Cell, 72(6):827–34.
[18] Lorenz J, Seebach E, Hackmayer G, Greth C, Bauer RJ, Kleinschmidt K, et al (2014). Melanocortin 1 receptor-signaling deficiency results in an articular cartilage phenotype and accelerates pathogenesis of surgically induced murine osteoarthritis. PLoS One, 9(9): e105858.
[19] Böhm M, Robert C, Malhotra S, Clément K, Farooqi S (2025). An overview of benefits and risks of chronic melanocortin-1 receptor activation. J Eur Acad Dermatol Venereol, 39(1):39–51.
[20] Behn A, Brendle S, Ehrnsperger M, Zborilova M, Grupp TM, Grifka J, et al (2025). Filtered and unfiltered lipoaspirates reveal novel molecular insights and therapeutic potential for osteoarthritis treatment: a preclinical in vitro study. Front Cell Dev, 13:1534281.
[21] Haskell-Luevano C, Hendrata S, North C, Sawyer TK, Hadley ME, Hruby VJ,Dickinson C, Gantz I (1997). Discovery of prototype peptidomimetic agonists at the human melanocortin receptors MC1R and MC4R. J Med Chem, 40(14):2133–9.
[22] Stanisz H, Seifert M, Tilgen W, Vogt T, Rass K (2011). Reciprocal responses of fibroblasts and melanocytes to α-MSH depending on MC1R polymorphisms. Dermatoendocrinol, 3(4):259–65.
[23] Beaumont KA, Shekar SL, Newton RA, James MR, Stow JL, Duffy DL, et al (2007). Receptor function, dominant negative activity and phenotype correlations for MC1R variant alleles. Hum Mol Genet, 16(18):2249–60.
[24] Glasson SS, Chambers MG, Van Den Berg WB, Little CB (2010). The OARSI histopathology initiative - recommendations for histological assessments of osteoarthritis in the mouse. Osteoarthritis Cartilage, 18:Suppl 3:S17-23.
[25] Ehrnsperger M, Taheri S, Pann P, Schilling AF, Grässel S (2024). Differential effects of alendronate on chondrocytes, cartilage matrix and subchondral bone structure in surgically induced osteoarthritis in mice. Sci Rep, 14(1):25026.
[26] Bankhead P, Loughrey MB, Fernández JA, Dombrowski Y, McArt DG, Dunne PD, et al (2017). QuPath: Open source software for digital pathology image analysis. Sci Rep, 7(1):16878.
[27] Jackson MT, Moradi B, Zaki S, Smith MM, McCracken S, Smith SM, et al (2014). Depletion of protease-activated receptor 2 but not protease-activated receptor 1 may confer protection against osteoarthritis in mice through extracartilaginous mechanisms. Arthritis Rheumatol (Hoboken, NJ), 66(12):3337–48.
[28] Pann P, Kalke P, Maier V, Schäfer N, Clausen-Schaumann H, Schilling AF, et al (2025). Decoding the impact of exercise and αCGRP signaling on murine post-traumatic osteoarthritis progression. Arthritis Res Ther, 27(1):129.
[29] Rösch G, Muschter D, Taheri S, El Bagdadi K, Dorn C, Meurer A, et al (2022). β2-Adrenoceptor Deficiency Results in Increased Calcified Cartilage Thickness and Subchondral Bone Remodeling in Murine Experimental Osteoarthritis. Front Immunol, 12: 801505.
[30] Rösch G, El Bagdadi K, Muschter D, Taheri S, Dorn C, Meurer A, et al (2022). Sympathectomy aggravates subchondral bone changes during osteoarthritis progression in mice without affecting cartilage degeneration or synovial inflammation. Osteoarthritis Cartilage, 30(3):461–74.
[31] Muschter D, Fleischhauer L, Taheri S, Schilling AF, Clausen-Schaumann H, Grässel S (2020). Sensory neuropeptides are required for bone and cartilage

homeostasis in a murine destabilization-induced osteoarthritis model. Bone, 133:11518.

[32] Mei J, Schäfer N, Wei P, Kong Z, Li S, Pann P, et al (2025). Targeting Caspase-1 in osteoarthritis: multi-omics insights into the effects of VX-765 on human chondrocyte function and phenotype. Front Immunol, 16:1677801.

[33] Motulsky HJ, Brown RE (2006). Detecting outliers when fitting data with nonlinear regression - A new method based on robust nonlinear regression and the false discovery rate. BMC Bioinformatics, 7:123.

[34] Böhm M, Apel M, Lowin T, Lorenz J, Jenei-Lanzl Z, Capellino S, et al (2016) α-MSH modulates cell adhesion and inflammatory responses of synovial fibroblasts from osteoarthritis patients. Biochem Pharmacol, 116:89–99.

[35] Beaumont KA, Liu YY, Sturm RA (2009). Chapter 4: The Melanocortin-1 Receptor Gene Polymorphism and Association with Human Skin Cancer. Prog Mol Biol Transl Sci, 88(C):85–153.

[36] Haubruck P, Pinto MM, Moradi B, Little CB, Gentek R (2021). Monocytes, Macrophages, and Their Potential Niches in Synovial Joints - Therapeutic Targets in Post-Traumatic Osteoarthritis? Front Immunol, 12:763702.

[37] Platzer H, Trauth R, Nees TA, Tripel E, Gantz S, Schiltenwolf M, et al (2022). CD8+ T Cells in OA Knee Joints Are Differentiated into Subsets Depending on OA Stage and Compartment. J Clin Med, 11(10):2814.

[38] Han Z, Wang K, Ding S, Zhang M (2024). Cross-talk of inflammation and cellular senescence: a new insight into the occurrence and progression of osteoarthritis. Bone Res, 12(1):69.

[39] Liu Y, Zhang Z, Li T, Xu H, Zhang H (2022). Senescence in osteoarthritis: from mechanism to potential treatment. Arthritis Res Ther, 24(1):174.

[40] Getting SJ, Kaneva M, Bhadresa Y, Renshaw D, Leoni G, Patel HB, et al (2009). Melanocortin peptide therapy for the treatment of arthritic pathologies. ScientificWorldJournal, 9:1394–414.

[41] Kaneva MK, Kerrigan MJP, Grieco P, Curley GP, Locke IC, Getting SJ (2012). Chondroprotective and anti-inflammatory role of melanocortin peptides in TNF-α activated human C-20/A4 chondrocytes. Br J Pharmacol, 167(1):67–79.

[42] Can VC, Locke IC, Kaneva MK, Kerrigan MJP, Merlino F, De Pascale C, et al (2020). Novel anti-inflammatory and chondroprotective effects of the human melanocortin MC1 receptor agonist BMS-470539 dihydrochloride and human melanocortin MC3 receptor agonist PG-990 on lipopolysaccharide activated chondrocytes. Eur J Pharmacol, 872:172971.

[43] Capsoni F, Ongari AM, Lonati C, Accetta R, Gatti S, Catania A (2015). α-Melanocyte-stimulating-hormone (α-MSH) modulates human chondrocyte activation induced by proinflammatory cytokines. BMC Musculoskelet Disord, 16(1):154.

[44] Dilley JE, Bello MA, Roman N, McKinley T, Sankar U (2023). Post-traumatic osteoarthritis: A review of pathogenic mechanisms and novel targets for mitigation. Bone Reports, 18:101658.

[45] Yudoh K, Nguyen van T, Nakamura H, Hongo-Masuko K, Kato T, Nishioka K (2005). Potential involvement of oxidative stress in cartilage senescence and development of osteoarthritis: oxidative stress induces chondrocyte telomere instability and downregulation of chondrocyte function. Arthritis Res, 7(2):R380-91.

[46] Vun J, Iqbal N, Jones E, Ganguly P (2023). Anti-Aging Potential of Platelet Rich Plasma (PRP): Evidence from Osteoarthritis (OA) and Applications in Senescence and Inflammaging. Bioeng (Basel, Switzerland), 10(8):987.

[47] Olivieri F, Prattichizzo F, Grillari J, Balistreri CR (2018). Cellular Senescence and Inflammaging in Age-Related Diseases. Mediators Inflamm, 2018:9076485.

[48] Guan J, Li Y, Ding L-B, Liu G-Y, Zheng X-F, Xue W, et al (2019). Synovial Fluid Alpha-Melanocyte-stimulating Hormone May Act as a Protective Biomarker for Primary Knee Osteoarthritis. Discov Med, 27(146):17–26.

[49] Liu T, Yao Z, He M, Tian C (2015). Synovial fluid α-MSH levels are inversely correlated with articular cartilage degeneration in anterior cruciate ligament deficient knees. Clin Lab, 61(8):965–71.

[50] Liu G, Chen Y, Wang G, Niu J (2016). Decreased synovial fluid α-melanocyte-stimulating-hormone (α-MSH) levels reflect disease severity in patients with posttraumatic ankle osteoarthritis. Clin Lab, 62(8):1491–500.

[51] Martin JA, Buckwalter JA (2002). Aging, articular cartilage chondrocyte senescence and osteoarthritis. Biogerontology, 3(5):257–64.

[52] Jin X, Wang BH, Wang X, Antony B, Zhu Z, Han W, et al (2017). Associations between endogenous sex hormones and MRI structural changes in patients with symptomatic knee osteoarthritis. Osteoarthritis Cartilage, 25(7):1100–6.

[53] Diekman BO, Loeser RF (2024). Aging and the emerging role of cellular senescence in osteoarthritis. Osteoarthritis Cartilage, 32(4):365–71.